Hindawi Publishing Corporation
Journal of Spectroscopy
Volume 2013, Article ID 491716, 6 pages
http://dx.doi.org/10.1155/2013/491716

Research Article

Fabrication of Ag:TiO_2 Nanocomposite Thin Films by Sol-Gel Followed by Electron Beam Physical Vapour Deposition Technique

Manish Kumar,[1] Krishna Kumar Parashar,[1] Sushil Kumar Tandi,[1] Tanuj Kumar,[2] D. C. Agarwal,[2] and Abhishek Pathak[3]

[1] *Department of Physics, Central University of Rajasthan, NH-8, Kishangarh 305801, India*
[2] *Inter University Accelerator Centre, Aruna Asaf Ali Marg, New Delhi 110067, India*
[3] *Ajay Kumar Garg Engineering College, Adhyatmik Nagar, Ghaziabad 201009, India*

Correspondence should be addressed to Manish Kumar; manishbharadwaj@gmail.com

Received 31 May 2013; Accepted 16 July 2013

Academic Editor: Yogendra Mishra

Ag:TiO_2 nanocomposite films have been synthesized by sol-gel method followed by electron beam physical vapour deposition. Targets for this deposition were prepared by a hydraulic press using a powder containing Ag and TiO_2 prepared by sol-gel technique. Microstructure, surface, and plasmonic properties of nanocomposite films were studied using glancing angle X-ray diffractometer, atomic force microscopy, field emission secondary electron microscopy, and UV-Vis spectroscopy. Microstructural study reveals that Ag nanoparticles are embedded in TiO_2 matrix consisting of mixed phases of anatase and rutile. Size estimation using Scherrer formula reveals that average crystallite size of Ag nanoparticles is 23 nm. Surface morphological studies indicate that deposited films are uniform and intact to the substrate and have very low value of root mean square roughness. Optical studies exhibit a surface plasmon resonance induced absorption band in visible region, which is the characteristic feature of Ag nanoparticles. The intensity of this absorption band is found to increase with the increase in deposition time. Multiple peaks observed in absorption band were explained using the concepts of extended Mie scattering. Preliminary experiments also suggested that these nanocomposite films exhibit promising photocatalytic properties, which can be used for water treatment.

1. Introduction

Plasmonic nanocomposites have been recently found to be the centre of attraction for their potential use in photocatalytic, nanosensing and optoelectronic and biomedical applications [1–6]. For example, Au nanoparticles of 3–8 nm diameters have been shown to tune the catalytic properties [1, 2]. Along with acting as an interface with the nanoscale, plasmonic nanocomposites can also change light-matter interactions at a very fundamental level. The possibility to confine light in subwavelength mode volume cavities has shown many optical processes that benefit from high optical quality factors and ultrasmall electromagnetic mode volumes [3]. This is the reason why plasmonic nanocomposites can be used to enhance a range of nonlinear processes in ultracompact device geometries, modify the temporal and spatial properties of light emitters, control both near and far field thermal radiation pathways, and manipulate light using new optical materials with engineered refractive indices [3]. Kumar et al. have shown plasmonic and nonlinear optical properties in Ag:ZrO_2 plasmonic nanocomposites [5]. Akhavan reported interesting antibacterial activities of Ag-TiO_2/Ag/a-TiO_2 nanocomposite thin film photocatalysts under solar light irradiation [6]. These applications are, in general, possible due to the unique plasmonic properties of nanocomposites, which explicitly depend on the size, shape, density, and distribution of noble metal nanoparticles in the nanosize domain along with the dielectric properties of a matrix [7]. Plasmonic properties arise due to collective excitation of free electrons, commonly known as surface plasmon resonances (SPRs). Tailoring of plasmonic properties via the engineering of spectral location, peak intensity,

and peak width of SPR has been theoretically [8, 9] as well as experimentally reported in nanocomposites consisting of noble metal nanoparticles embedded inside [10–13] or dispersed at [14, 15] the surface of polymers/dielectric oxides by controlling the size, shape, and interparticle spacing of the metal NPs and the dielectric constant of the embedding matrix.

As far as the selection of synthesis technique is concerned, there are two kinds of approaches for growing the nanostructures: "top down" and "bottom up." In the top down approach, low energy ions induced nanostructuring has found recent interests [15–18], on the other hand more explored "bottom up" approach is utilised in variety of techniques, that is, sol-gel [7], chemical reduction [10], physical vapour deposition [19], atom beam sputtering [20–22], magnetron cosputtering [23], and so forth. By controlling the synthesis parameters, it is possible to grow noble nanostructures (e.g., nanoprisms, nanorods, or nanoshells), which is particularly important to integrate such metal nanoparticles into biological systems, which are being utilized for biodiagnostics, biophysical studies, and medical therapy [24].

Among the different plasmonic nanocomposites, Ag:TiO_2 nanocomposites have been particularly interesting due to their extremely interesting properties [25–33]. Among these, photo degradation of textile dyes, methylene blue and direct azo dyes [25–27], photochromic properties [28, 29], purification of water [30], photoelectrochemical hydrogen production from the water methanol decomposition [31], and "special heat mirror" with high transparency in the near UV region [32] can be named as few. In most of the catalytic studies metal nanoparticles are dispersed on an oxide surface. Such kinds of structures result in exposing metal to both the reactants and the surrounding medium. Corrosion or dissolution of the noble metal particles during the operation of a photocatalytic reaction is likely to limit the use of noble metal such as Ag and Au. In particular, metal nanoparticles deposited on TiO_2 nanostructures undergo Fermi level equilibration following the UV excitation and enhance the efficiency of charge-transfer process [33]. However there are very limited reports, which deal the photocatalytic properties of embedded systems. Nanocomposites of embedded nanoparticles configurations are considered to be better for stability point of view. Keeping in our consideration that compared to other synthesis procedures, electron beam physical vapour deposition (EBPVD) is an ideal choice for high quality films with uniform thickness, we selected this technique to fabricate the Ag:TiO_2 nanocomposite films. Hence in this work, we presented the fabrication process and microstructural and plasmonic properties of fabricated Ag:TiO_2 nanocomposite thin films.

2. Experimental

The processing steps of nanocomposite thin films are summarily schematically shown in Figure 1. Process to form a polymeric sol is followed from our earlier works [34, 35]. Sol of 0.1 M was prepared by mixing titanium isopropoxide (M/s STREM chemicals) precursor in 2-propanol solvent and stirred for 6 h. HCl was mixed in the appropriate quantity for controlling the hydrolysis rate. This solution was stirred for 18 h keeping temperature constant at 35°C and humidity between 40% and 50%. In this sol, $AgNO_3$ (M/s Qualigens Fine Chemicals) was mixed maintaining the silver precursor concentration as 0.1 M was added and stirring continued for another 6 h. Thermal annealing was carried out at 150°C in static air using a programmable muffle furnace (M/s Metrex Scientific Instruments), keeping the heating rate constant at 2.5°C/min, and powder of Ag:TiO_2 was obtained. Using a hydraulic press and putting 8-ton weight, pellets of 1 cm diameter and 3 mm thickness were prepared and used as the targets for EBPVD system. In the newly installed EBPVD system (M/s Hind High Vacuum) at *Central University of Rajasthan*, chemically cleaned glass slides were kept in holder, which works as a anode and bombarded with electron beam generated by Tungsten filament inside a chamber having vacuum ~ 2×10^{-6} Torr. The current is kept constant during deposition as 100 mA and voltage as 5 kV. For getting different thickness of the nanocomposite films, deposition time was used as 5 min and 10 min. Finally the deposited films were annealed at 400°C for 2 h.

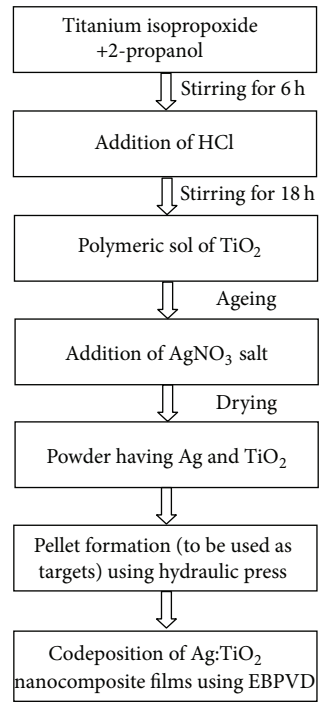

Figure 1: Flow chart of various synthesis steps of Ag:TiO_2 nanocomposite thin films.

The morphology of the films and size of Ag particles were studied using field emission scanning transmission electron microscopy (FESEM) machine of Zeiss model. Glancing angle X-ray diffraction (GAXRD) patterns were recorded in the range of 20–60° with an X-ray diffractometer (Bruker, D8 Advanced). The surface topography of the samples was examined using nanoscope IIIa atomic force microscope (AFM) in contact mode conditions. UV-visible absorption

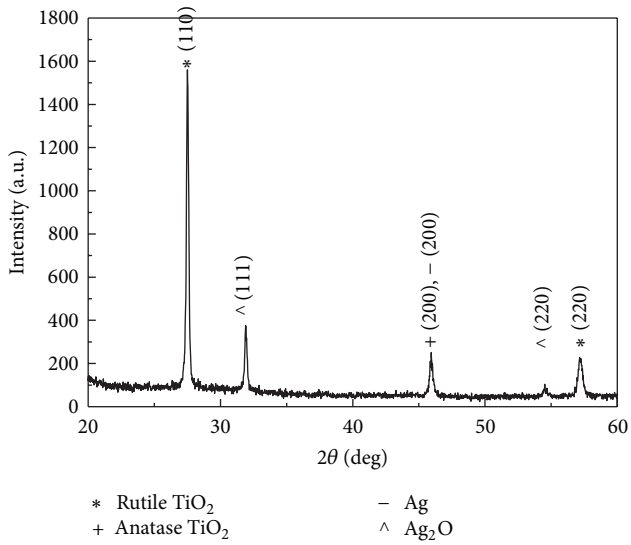

FIGURE 2: Glancing angle X-ray diffraction pattern of Ag:TiO_2 nanocomposite thin film annealed at 400°C. (Different phases are indexed as different symbols: * for rutile TiO_2, + for anatase TiO_2, – for Ag, and ^ for Ag_2O.)

spectra of samples were recorded using a Hitachi U3300 dual beam spectrophotometer.

3. Results and Discussion

Figure 2 shows the XRD pattern of Ag:TiO_2 thin film sintered at 400°C, recorded in the 2θ region of 20–60°. The pattern shows different diffraction peaks at 27.13°, 32.1°, 46.17°, 54.2°, and 57° 2θ values, which are identified corresponding to the different crystallographic planes: rutile TiO_2 (110), Ag_2O (111), anatase TiO_2 (200) and Ag (200), Ag_2O (220), and rutile TiO_2 (220), respectively. All these diffraction peaks are indexed in Figure 2. It is interesting to have the presence of Ag_2O peaks in nanocomposite films because it is understood that oxides of Ag are decomposed into Ag at ~400°C [13]. Here, it is possible that with time a layer of oxide grows as shell to Ag nanoparticle cores which are at surface. For the estimation of size of Ag nanoparticles, the average crystallite size calculation is done using the Scherrer equation [36]:

$$t = \frac{k\lambda}{B\cos\theta}, \tag{1}$$

where λ = wavelength of X ray source = 1.54 Å, and B = FWHM (full width at half maximum) corresponding to XRD peaks. Using this equation crystalline sizes are estimated as 40.17 nm for TiO_2 and 23.7 nm for Ag nanoparticle.

Surface features of nanocomposites have been studied by AFM in contact mode to examine the quality of film deposition on glass substrate. The AFM image of thin film, shown in Figure 3(a), confirms that there is uniform deposition of Ag:TiO_2 on the glass substrate. The root mean square roughness was also calculated and found to be as 11.23 nm, which shows that good quality of films was achieved by the present technique.

Morphological study of the nanocomposite sample has also been investigated using FESEM imaging. It is evident that this technique is more reliable as secondary electrons, generated at near surface regions, provides accurate topographic information of sample. Also, the different interaction of primary electron beam with the surface elements provides better insight evolution of different nanostructures. The FESEM image of Ag:TiO_2 thin film, recorded at 154 kx magnification using FIB probe at 30 kV and emission current as 2 nA, is shown in Figure 3(b), which reveals that film is uniform and densely packed and has particle size in the range of 20–40 nm. This particle size estimation is in close agreement with the average particle size estimated using the Scherrer formula as mentioned earlier.

The spectral variation in optical absorbance spectrum obtained from the Ag:TiO_2 nanocomposite thin films is shown in Figure 4. The two curves in the absorption spectra are corresponding to two different thicknesses of the nanocomposite films prepared for deposition time as 5 min and 10 min. These spectra show that there is a significant absorption band in visible range whose intensity increases with the increase in thickness of the nanocomposite films. This absorption band is because of the SPR of the Ag nanoparticles evolved in the nanocomposite thin films. The absorption band in case of 5 min deposition time consists of four distinct peaks situated at wavelengths 380 nm, 439 nm, 516 nm, and 665 nm. There can be two reasons for these four peaks, first an effect of thickness and second different modes of SPR. We will discuss both one by one. First, we consider it because of the thickness effect; in this case depending on the relation of product of thickness and refractive index to integral multiples of path difference, an interference pattern is obtained, which is usually seen as multiple loops in transmittance and reflectance values. In such case, the number of loops increases in a fixed wavelength region if thickness of film is increased. Since, in present case, we did not observe increase in number of loops, we can disregard the thickness effect. Now if we consider the different modes of SPR, it is well known that depending on the average size and multiple interactions, there can be different modes of SPR band.

Theoretical analysis of these spectra can be done using generalized Mie scattering theory or using the different effective theories [37, 38]. Size dependence of dielectric constant of noble metals is determined by a free path effect [37, 39], which is based upon the Drude-Sommerfeld theory and gives an expression for a size dependent collision frequency of conduction electrons. The particle surface is considered as a scatterer of conduction electrons. The appropriate mean free path L_{sphere} of an electron, disregarding its coupling to the Fermi liquid, is calculated to be equal to the particle size (r). Provided that all scattering mechanisms of the conduction electrons in a spherical particle are independent of one another, the effective collision frequency ω_D is given by $\omega_D = \omega_{D,\text{bulk}} + \nu_F/r$, where ν_F is Fermi velocity and $\omega_{D,\text{bulk}}$ is collision frequency of electrons in bulk metal (for Ag $\nu_F = 1.4 \times 10^6$ ms^{-1} and $\omega_{D,\text{bulk}} = 2.7 \times 10^{13}$ s^{-1}). ω_D is assumed to

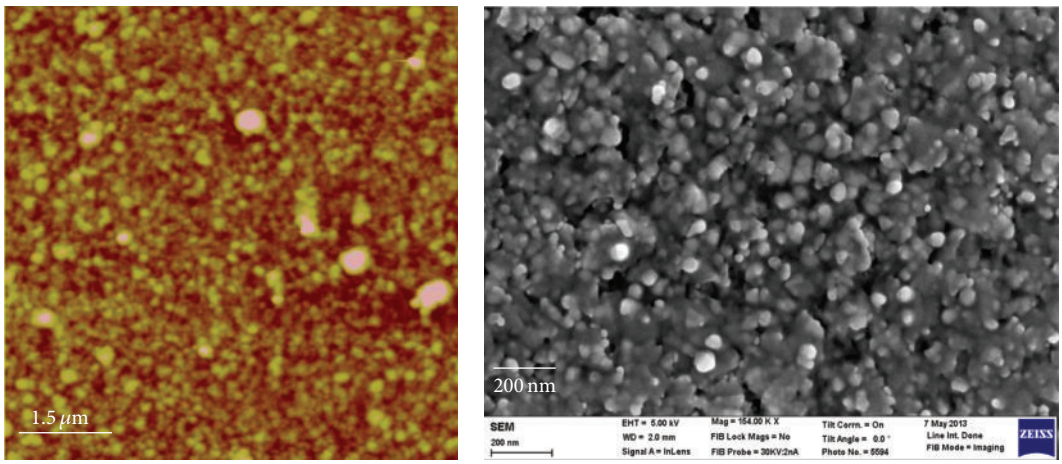

(a) (b)

Figure 3: (a) Surface topography of Ag:TiO_2 nanocomposite thin films recorded by AFM in contact mode recorded in scan area 7.5 μm × 7.5 μm. (b) Surface morphology of Ag:TiO_2 nanocomposite thin films recorded by FESEM using 30 kV electron beam.

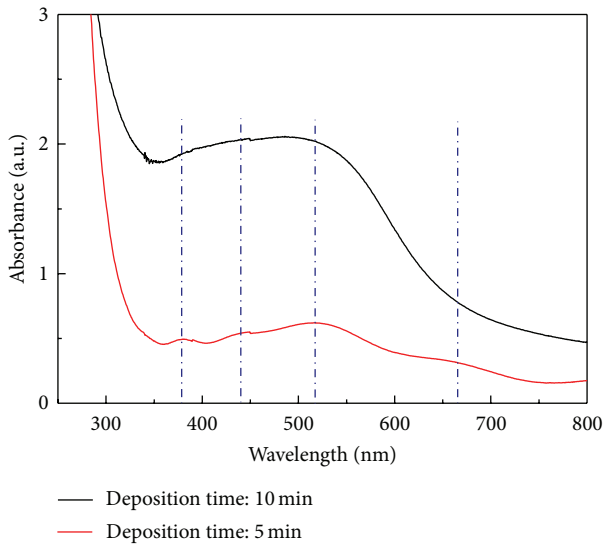

Figure 4: Absorption spectra of Ag:TiO_2 nanocomposite thin film prepared by deposition time 5 min and 10 min.

be isotropic. The correction of collision frequency yields size dependent dielectric functions as follows:

$$\varepsilon(\omega, r) = \varepsilon_1(\omega) + i\varepsilon_2(\omega, r) = \varepsilon_1(\omega) + i\left[\varepsilon_{2,\text{bulk}}(\omega) + \eta\frac{\omega_p^2}{\omega^3}\left(\frac{v_F}{r}\right)\right], \quad (2)$$

where ε_1 and ε_2 are the real and imaginary parts of dielectric constant of metal particles, ω_p is the Drude plasma frequency (for silver $\omega_p = 1.46 \times 10^{16}\,\text{s}^{-1}$), and parameter η is a phenomenological factor that includes other kinds of interactions: electron-electron, electron-phonon, and electron-defects. In Figure 5(a), spectral dependence of ε_2 on different size variation (from $r = 2.5$ nm to $r = 20$ nm) of Ag nanoparticles is shown. The values of ε_2 for bulk Ag are also compared, which are adopted from the reports by Johnson and Christy [40]. By using the size dependent dielectric functions of metal, Mie's solutions are simplified in *quasi-static regime*. In *quasi-static regime* (valid for particles size $r \ll \lambda$), retardation effects of the electromagnetic field over the particle diameter are negligible, so the generally multipolar excitations of Mie's theory are restricted to the dipolar electric mode [37]. Absorption coefficient (K) for a system of spherical metal particles embedded in a transparent dielectric matrix, where the imaginary part of the relative complex electric permittivity approaches zero (Im $\varepsilon_m \to 0$), is then given as [37]

$$K = \frac{18\pi C\varepsilon_m^{3/2}(\omega)\,\varepsilon_2(\omega, r)}{\lambda\left(\left(\varepsilon_1(\omega) + 2\varepsilon_m(\omega)\right)^2 + \varepsilon_2^2(\omega, r)\right)}, \quad (3)$$

where C is volume concentration of embedded metal particles. From (3), it is evident that maxima in absorption can be obtained if condition $\varepsilon_1(\omega) = -2\varepsilon_m(\omega)$ is fulfilled. This condition gives the criterion of SPR, corresponding to the first order mode of scattering of light by a metallic sphere at a wavelength λ_{SP} (surface plasmon wavelength) in visible or near UV. In this condition, the dipole moment and local field in the vicinity of a given metallic particles will grow resonantly to values that overcome the field of the incident wave by many orders of magnitudes. Theoretical Mie scattering intensities for Ag particles of various sizes in matrix (for fixed refractive index = 1.7) have been calculated using the software *MIEPLOT v4.0.0.1* [41] and presented here in Figure 5(b) to illustrate the dramatic effect of size on plasmonic response. This plot gives hint that multiple peaks in SPR induced absorption band can be obtained if the frequencies of particle sizes are centred on some definite values. Such kind of distribution is usually called multimodal distribution.

Here, it would be appropriate to discuss that the spectral position observed in present case is red-shifted to the usual

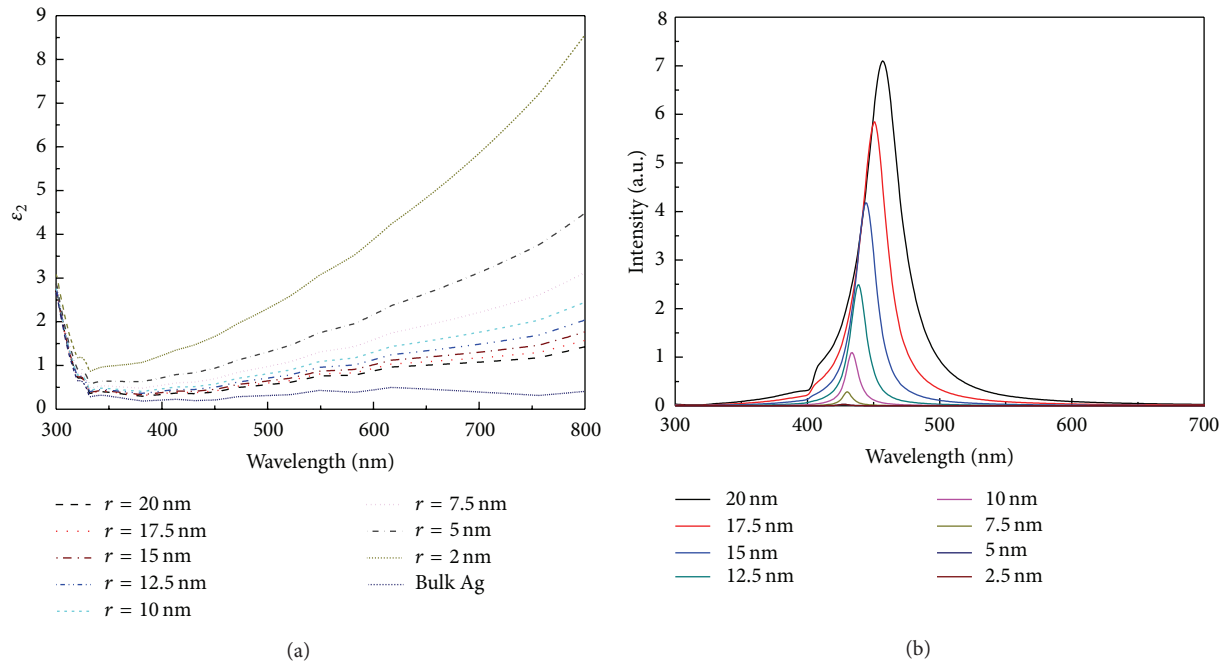

FIGURE 5: Theoretically estimated size dependent variation in imaginary part of dielectric constant of Ag nanoparticles (a) and Mie scattering intensity at scattering angle 180°, for the fixed refractive index of medium as 1.7 (b).

position of SPR of Ag nanoparticles nearby 400 nm. The obvious reason behind this red shift is the higher refractive matrix TiO_2 in comparison to SiO_2 and other dielectric oxides. In present case, different deposition time induces different thickness of the nanocomposite films which means different volume fraction of metal component in nanocomposite films. The broadness of peak can be associated with two possible reasons: first oxide shell formation during thermal treatment and second asymmetric shape of silver nanoparticles. It is possible that both of these reasons are applicable here. These nanocomposite films have been initially tested for photocatalytic application, which shows enhancement in degradation efficiency of organic dyes (methylene blue) when compared with TiO_2 films. Detailed work in this direction is in process.

4. Conclusion

This work reports successful fabrication of Ag:TiO_2 NC thin films potentially interesting for photocatalytic applications. The synthesis technique is based on the sol-gel process followed by EBPVD. FESEM and XRD independently revealed the size of Ag nanoparticles close to 23 nm. Microstructural study further provided the information of matrix as a mixed phase of rutile and anatase when nanocomposites are annealed at 400°C. FESEM imaging shows that deposition of nanocomposite on the substrate was uniform and densely packed. Optical studies ensured the formation of Ag nanoparticles by exhibiting an SPR induced absorption band in visible region whose intensity can be increased by increasing the deposition duration.

Acknowledgments

The authors acknowledge the cooperation of Dr. D. K. Avasthi in allowing the optical and surface characterizations of the samples at IUAC, New Delhi, and the help of Mr. Gaurav Kaushik (Karl Zeiss, India) in FESEM imaging of samples.

References

[1] T. Hirakawa and P. V. Kamat, "Charge separation and catalytic activity of Ag@TiO_2 core-shell composite clusters under UV-irradiation," *Journal of the American Chemical Society*, vol. 127, no. 11, pp. 3928–3934, 2005.

[2] Z. Yang, R. Wu, and D. W. Goodman, "Structural and electronic properties of Au on TiO_2(110)," *Physical Review B*, vol. 61, no. 20, pp. 14066–14071, 2000.

[3] J. A. Schuller, E. S. Barnard, W. Cai, Y. C. Jun, J. S. White, and M. L. Brongersma, "Plasmonics for extreme light concentration and manipulation," *Nature Materials*, vol. 9, no. 3, pp. 193–204, 2010.

[4] R. Singh, E. Smirnova, A. J. Taylor, J. F. O'Hara, and W. Zhang, "Optically thin terahertz metamaterials," *Optics Express*, vol. 16, no. 9, pp. 6537–6543, 2008.

[5] M. Kumar, S. Sandeep, G. Kumar, Y. K. Mishra, R. Philip, and G. B. Reddy, "Plasmonic and nonlinear optical absorption properties of Ag:ZrO_2 nanocomposite thin films," *Plasmonics*, 2013.

[6] O. Akhavan, "Lasting antibacterial activities of Ag-TiO_2/Ag/a-TiO_2 nanocomposite thin film photocatalysts under solar light irradiation," *Journal of Colloid and Interface Science*, vol. 336, no. 1, pp. 117–124, 2009.

[7] M. Kumar, P. K. Kulriya, J. C. Pivin, and D. K. Avasthi, "Evolution and tailoring of plasmonic properties in Ag:ZrO_2

nanocomposite films by swift heavy ion irradiation," *Journal of Applied Physics*, vol. 109, no. 4, Article ID 044311, 2011.

[8] G. Kumar and V. K. Tripathi, "Anomalous absorption of surface plasma wave by particles adsorbed on metal surface," *Applied Physics Letters*, vol. 91, no. 16, Article ID 161503, 3 pages, 2007.

[9] G. Kumar, D. B. Singh, and V. K. Tripathi, "Surface enhanced Raman scattering of a surface plasma wave," *Journal of Physics D*, vol. 39, no. 20, pp. 4436–4439, 2006.

[10] M. Kumar and G. B. Reddy, "Effect of atmospheric exposure on the growth of citrate-capped silver nanoparticles," *Physica E*, vol. 42, no. 7, pp. 1940–1943, 2010.

[11] M. Kumar and G. B. Reddy, "Tailoring surface plasmon resonance in Ag:ZrO_2 nanocomposite thin films," *Physica E*, vol. 43, no. 1, pp. 470–474, 2010.

[12] Y. K. Mishra, S. Mohapatra, D. Kabiraj et al., "Synthesis and characterization of Ag nanoparticles in silica matrix by atom beam sputtering," *Scripta Materialia*, vol. 56, no. 7, pp. 629–632, 2007.

[13] M. Kumar and G. B. Reddy, "Ag:ZrO_2 nanocomposite thin films derived using a novel sol-gel technique," *Physica Status Solidi*, vol. 246, no. 10, pp. 2232–2237, 2009.

[14] Y. K. Mishra, R. Adelung, G. Kumar et al., "Formation of self-organized silver nanocup-type structures and their plasmonic absorption," *Plasmonics*, vol. 8, no. 2, pp. 811–815, 2013.

[15] U. B. Singh, D. C. Agarwal, S. A. Khan et al., "Engineering of hydrophilic and plasmonic properties of Ag thin film by atom beam irradiation," *Applied Surface Science*, vol. 258, no. 4, pp. 1464–1469, 2011.

[16] T. Kumar, M. Kumar, G. Gupta, R. K. Pandey, S. Verma, and D. Kanjilal, "Role of surface composition in morphological evolution of GaAs nano-dots with low-energy ion irradiation," *Nanoscale Research Letters*, vol. 7, article 552, 2012.

[17] T. Kumar, M. Kumar, S. Verma, and D. Kanjilal, "Fabrication of ordered ripple patterns on GaAs(100) surface using 60 keV Ar+ beam irradiation," *Surface Engineering*, 2013.

[18] I. Sulania, D. C. Agarwal, M. Kumar, M. Hussain, and D. K. Avasthi, "Low energy bombardment induced formation of Ge nanoparticles," *Advanced Materials Letters*, vol. 4, no. 6, pp. 402–407, 2013.

[19] D. K. Avasthi, Y. K. Mishra, D. Kabiraj, N. P. Lalla, and J. C. Pivin, "Synthesis of metal-polymer nanocomposite for optical applications," *Nanotechnology*, vol. 18, no. 12, Article ID 125604, 2007.

[20] M. Tiwary, N. K. Singh, S. Annapoorni et al., "Enhancement of photoluminescence in Er-doped Ag-SiO_2 nanocomposite thin films: a post annealing study," *Vacuum*, vol. 85, no. 8, pp. 806–809, 2011.

[21] Y. K. Mishra, S. Mohapatra, V. S. K. Chakravadhanula et al., "Synthesis and characterization of Ag-polymer nanocomposites," *Journal of Nanoscience and Nanotechnology*, vol. 10, no. 4, pp. 2833–2837, 2010.

[22] S. Mohapatra, Y. K. Mishra, J. Ghatak, D. Kabiraj, and D. K. Avasthi, "Surface plasmon resonance of Ag nanoparticles embedded in partially oxidized amorphous Si matrix," *Journal of Nanoscience and Nanotechnology*, vol. 8, no. 8, pp. 4285–4289, 2008.

[23] U. Schürmann, W. Hartung, H. Takele, V. Zaporojtchenko, and F. Faupel, "Controlled syntheses of Ag-polytetrafluoroethylene nanocomposite thin films by co-sputtering from two magnetron sources," *Nanotechnology*, vol. 16, no. 8, pp. 1078–1082, 2005.

[24] P. K. Jain, X. Huang, I. H. El-Sayed, and M. A. El-Sayed, "Review of some interesting surface plasmon resonance-enhanced properties of noble metal nanoparticles and their applications to biosystems," *Plasmonics*, vol. 2, no. 3, pp. 107–118, 2007.

[25] A. R. Malagutti, H. A. J. L. Mourão, J. R. Garbin, and C. Ribeiro, "Deposition of TiO_2 and Ag:TiO_2 thin films by the polymeric precursor method and their application in the photodegradation of textile dyes," *Applied Catalysis B*, vol. 90, no. 1-2, pp. 205–212, 2009.

[26] S. Senthilkumaar, K. Porkodi, R. Gomathi, A. Geetha Maheswari, and N. Manonmani, "Sol-gel derived silver doped nanocrystalline titania catalysed photodegradation of methylene blue from aqueous solution," *Dyes and Pigments*, vol. 69, no. 1-2, pp. 22–30, 2006.

[27] N. Sobana, M. Muruganadham, and M. Swaminathan, "Nano-Ag particles doped TiO_2 for efficient photodegradation of Direct azo dyes," *Journal of Molecular Catalysis A*, vol. 258, no. 1-2, pp. 124–132, 2006.

[28] K. Matsubara and T. Tatsuma, "Morphological changes and multicolor photochromism of Ag nanoparticles deposited on single-crystalline TiO_2 surfaces," *Advanced Materials*, vol. 19, no. 19, pp. 2802–2806, 2007.

[29] Y. Ohko, T. Tatsuma, T. Fujii et al., "Multicolour photochromism of TiO_2 films loaded with silver nanoparticles," *Nature Materials*, vol. 2, no. 1, pp. 29–31, 2003.

[30] M. Pratap Reddy, A. Venugopal, and M. Subrahmanyam, "Hydroxyapatite-supported Ag-TiO_2 as Escherichia coli disinfection photocatalyst," *Water Research*, vol. 41, no. 2, pp. 379–386, 2007.

[31] N. Alenzi, W.-S. Liao, P. S. Cremer et al., "Photoelectrochemical hydrogen production from water/methanol decomposition using Ag/TiO_2 nanocomposite thin films," *International Journal of Hydrogen Energy*, vol. 35, no. 21, pp. 11768–11775, 2010.

[32] Z. Wang, X. Cai, Q. Chen, and L. Li, "Optical properties of metal-dielectric multilayers in the near UV region," *Vacuum*, vol. 80, no. 5, pp. 438–443, 2006.

[33] M. Jakob, H. Levanon, and P. V. Kamat, "Charge distribution between UV-irradiated TiO_2 and gold nanoparticles: determination of shift in the Fermi level," *Nano Letters*, vol. 3, no. 3, pp. 353–358, 2003.

[34] M. Kumar and G. B. Reddy, "Effect of sol-age on the surface and optical properties of sol-gel derived mesoporous zirconia thin films," *AIP Advances*, vol. 1, no. 2, Article ID 022111, 10 pages, 2011.

[35] M. Kumar and G. B. Reddy, "A modified chemical route for synthesis of zirconia thin films having tunable porosity," *MRS Proceedings*, vol. 1074, 2008.

[36] C. Suryanarayan and M. G. Norton, *X-Ray Diffraction: A Practical Approach*, Plenum Press, New York, NY, USA, 1998.

[37] U. Kreibig and M. Vollmer, *Optical Properties of Metal Clusters*, Springer, New York, NY, USA, 1995.

[38] T. C. Choy, *Effective Medium Theory*, Clarendon Press, Oxford, UK, 1999.

[39] U. Kreibig, "Electronic properties of small silver particles: the optical constants and their temperature dependence," *Journal of Physics F*, vol. 4, no. 7, pp. 999–1014, 1974.

[40] P. B. Johnson and R. W. Christy, "Optical constants of the noble metals," *Physical Review B*, vol. 6, no. 12, pp. 4370–4379, 1972.

[41] http://www.philiplaven.com/mieplot.htm.